

Max Planck Institute
for Gravitational Physics
(Albert Einstein Institute)



VNIVERSITAT DE VALÈNCIA

Multi-Messenger Astrophysics in the Gravitational Wave Era

September 24 - October 25 2019,

Yukawa Institute for Theoretical Physics, Kyoto University

Universal relations of core-collapse supernova with gravitational waves

Alejandro Torres Forné

P. Cerdá-Durán, M. Obergaulinger, B Müller and J.A. Font

Phys. Rev. Lett. 123 (2019) no.5, 051102 arXiv:1902.10048

Outline

Introduction

- Motivation
- Core-collapse supernova (CCSN) signal



Universal relations

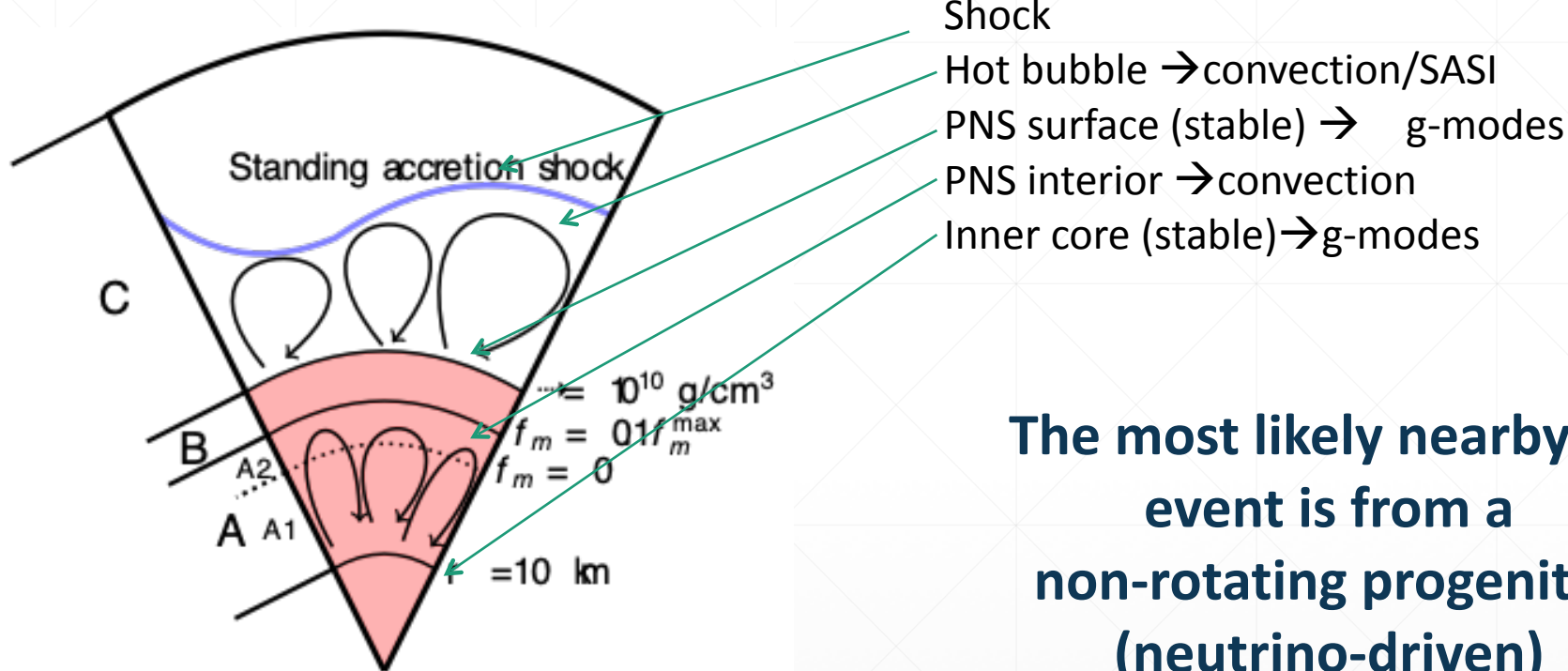
- Procedure
- Results
- Future work

Proto-neutron star mode analysis

- Origin
- Classification
- Comparison with simulations



Introduction - GW from CCSN

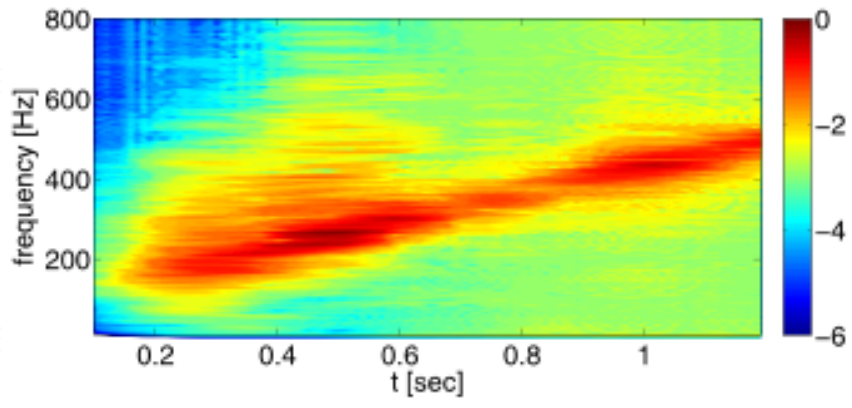


Andresen et al 2016

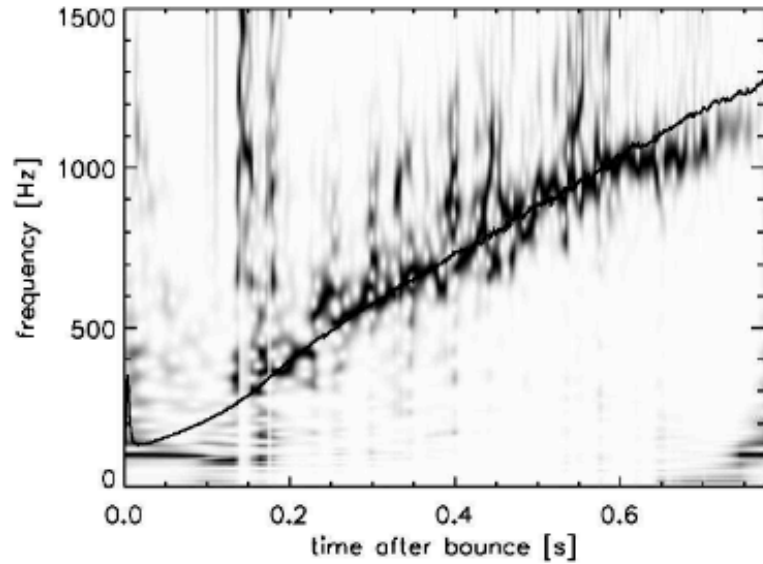
The most likely nearby CC event is from a non-rotating progenitor (neutrino-driven)

The proto-neutron star (PNS) is the source of most of the GW emission

Gravitational wave signal

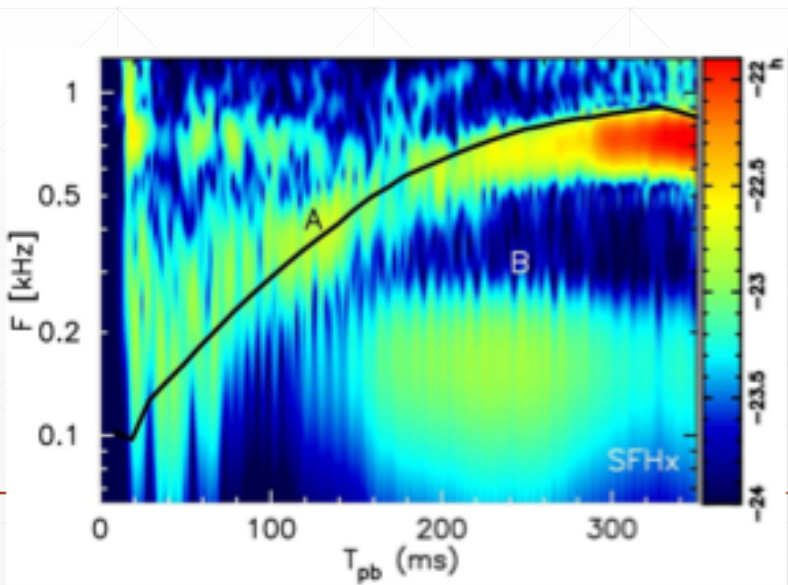


Müller et al 2012



Müller et al 2013

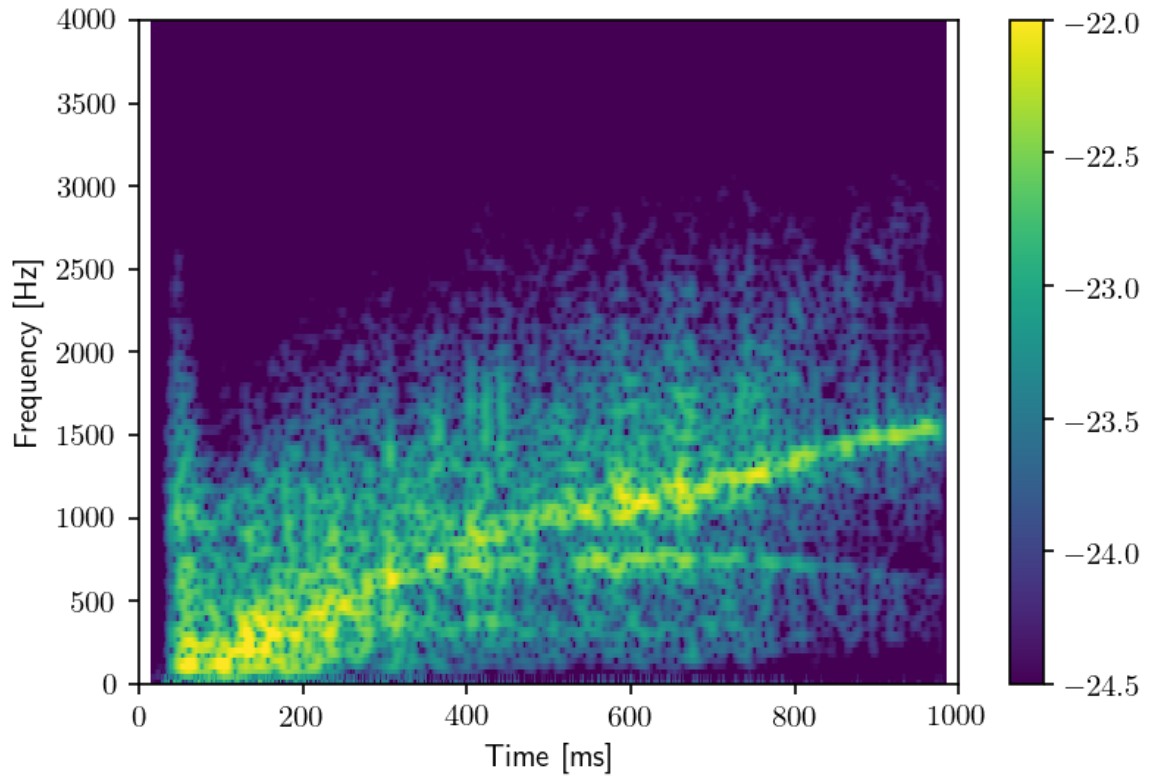
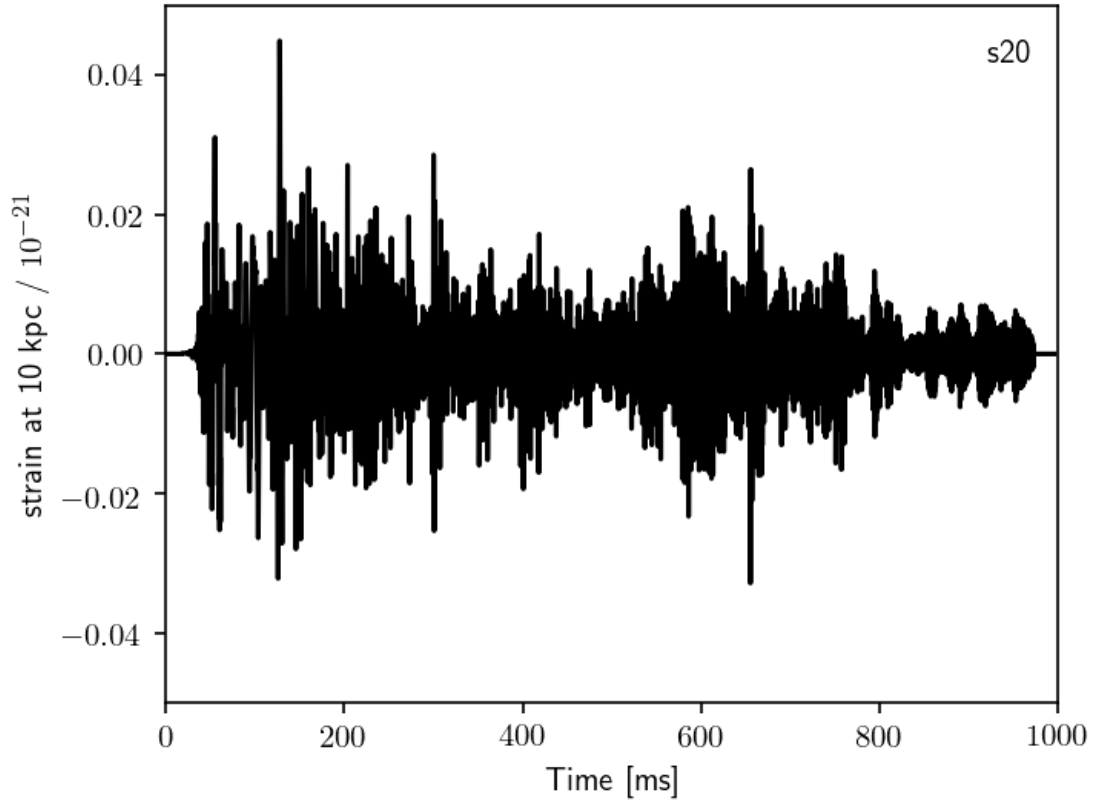
- Arches with raising frequency associated with g-modes of the PNS
- Observed systematically in all simulations (2D and 3D)
- If SASI is present, additional SASI modes.



Kuroda et al 2016

Numerical simulations

Obergaulinger M., Just O., Aloy M. Á., 2018, J. Phys.G. in press,



Motivation

Supernova modelling

- Sophisticated microphysics
- Computational challenges
- Progenitor uncertainties
- ...

GW observations & data analysis



Simulation
templates

Motivation

Supernova modelling

- Sophisticated microphysics
- Computational challenges
- Progenitor uncertainties
- ...

GW/mode frequency

- Surface gravity (M/R^2)
- Central density
- PNS surface temperature
- ...

GW observations & data analysis



Simulation templates
+ mode analysis

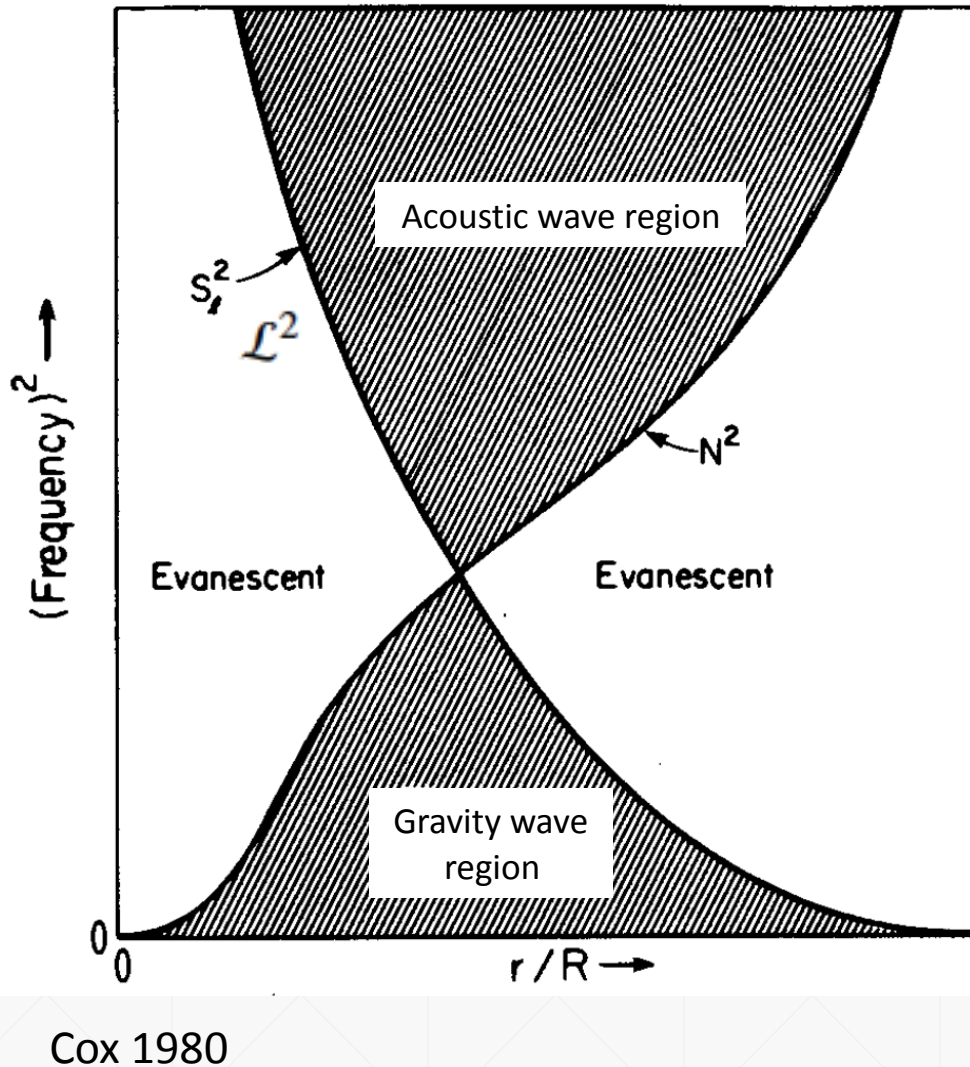
Phenomenological
parameterized
templates

Linear perturbation analysis

Linear perturbations of a spherical background

- Simplified background: Reisenegger & Goldreich 1992, Ferrari et al 2003, 2004, Passamonti et al 2005, Krüger et al 2015, Camelio et al 2017
- Background based on simulations (f, p and w modes): Sotani et al 2018
- Background from simulations + Cowling approximation: TF et al 2018a
- Background from simulations + lapse perturbations: Morozova et al 2018
- TF et al 2018b
 - Space-time perturbations (lapse and conformal factor)
 - Quadrupolar modes ($l=2$)
 - Quasi-radial ($l=0$) oscillations of deformed stars
 - Boundary conditions at the shock location
- **GREAT** code: [General Relativistic Eigenmode Analysis Tool](https://www.uv.es/cerdupa/codes/GREAT/). <https://www.uv.es/cerdupa/codes/GREAT/>

What are p/g/f modes?



N^2 : Brunt-Väisälä frequency

\mathcal{L}^2 : Lamb frequency

Acoustic wave region:

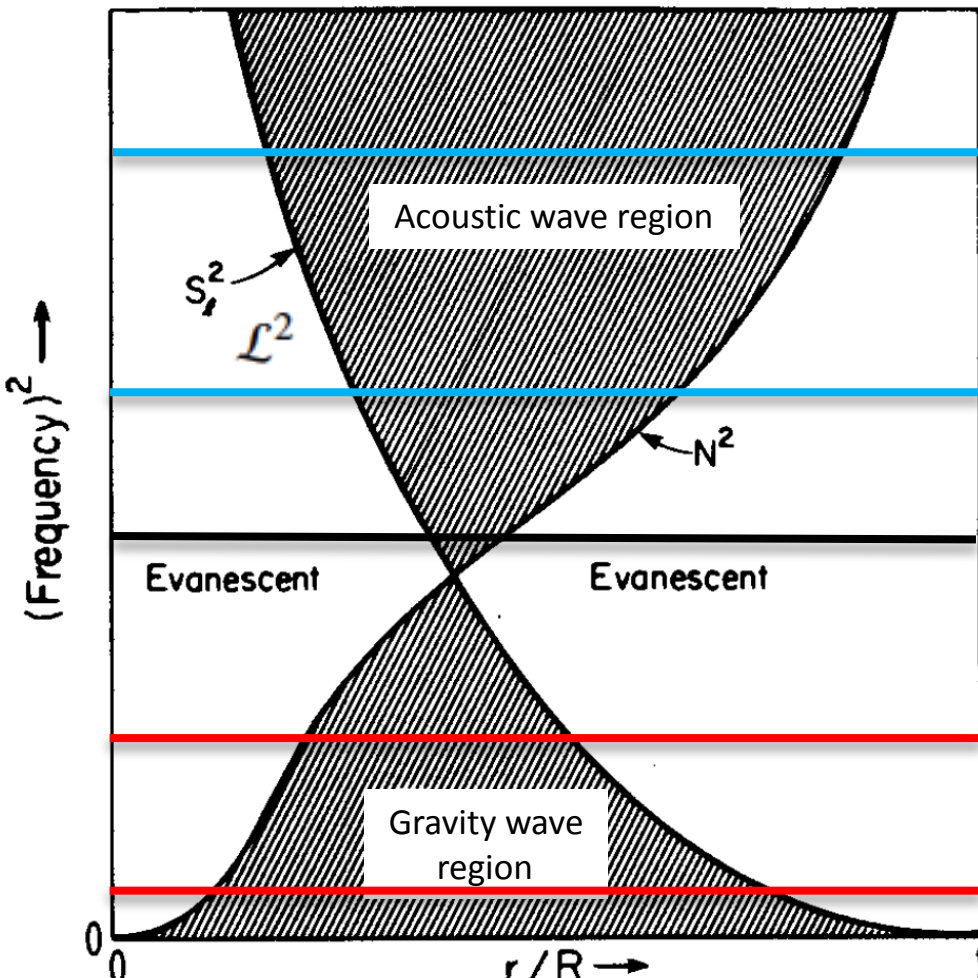
$$\sigma^2 > N^2, \mathcal{L}^2$$

Gravity wave region:

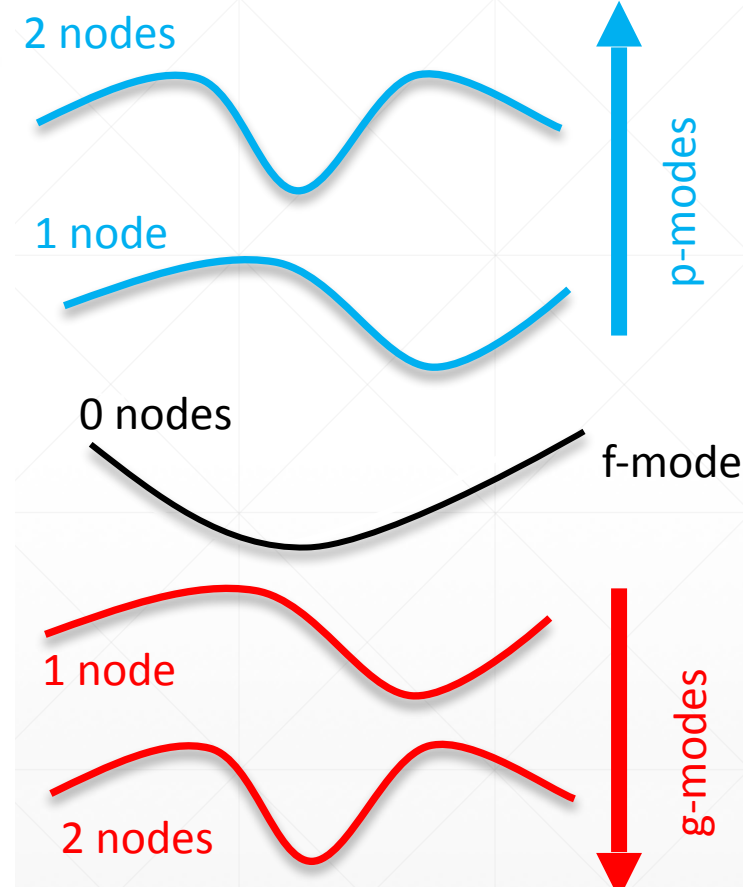
$$\sigma^2 < N^2, \mathcal{L}^2$$

Propagation diagram

What are p/g/f modes?

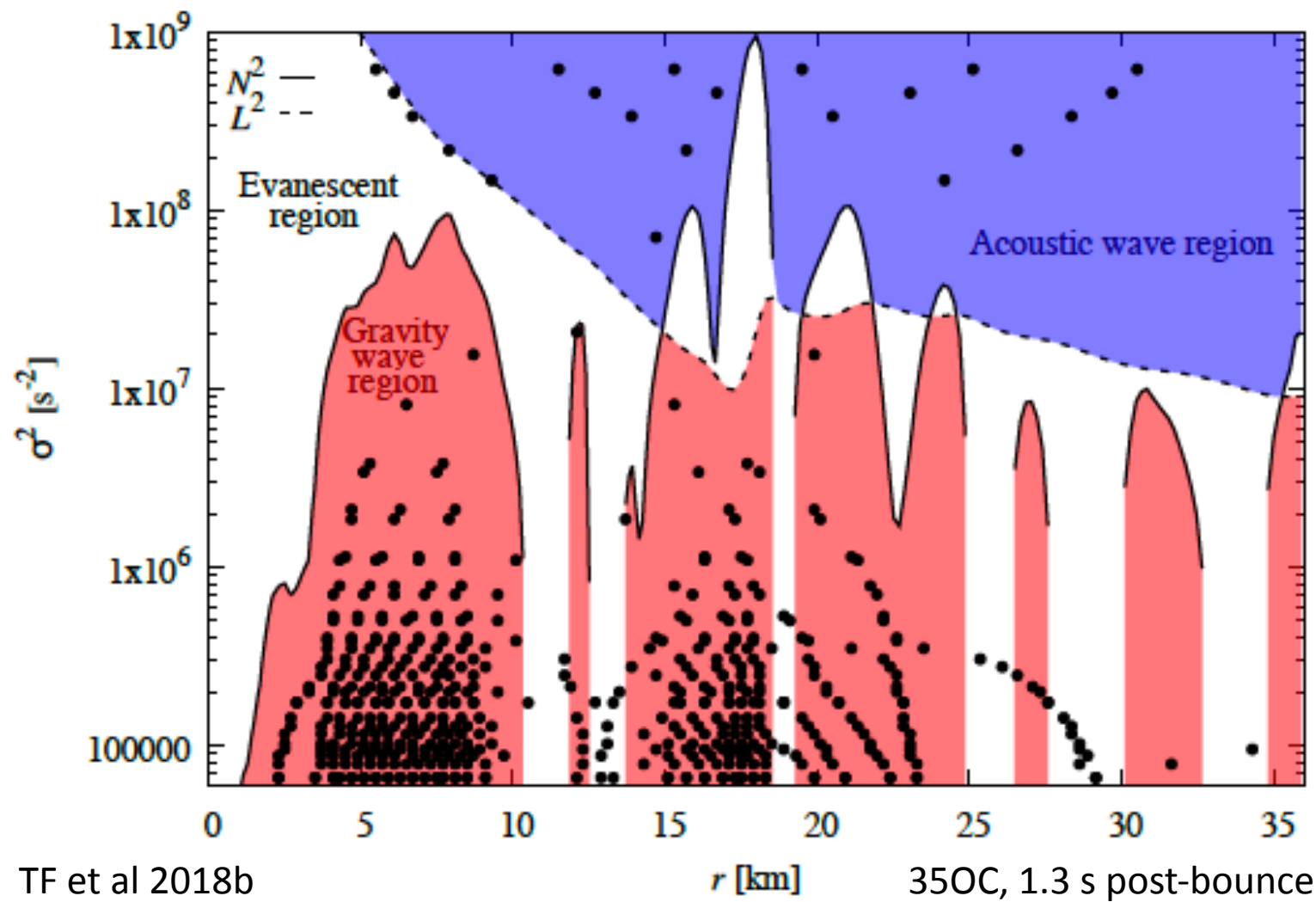


Cox 1980

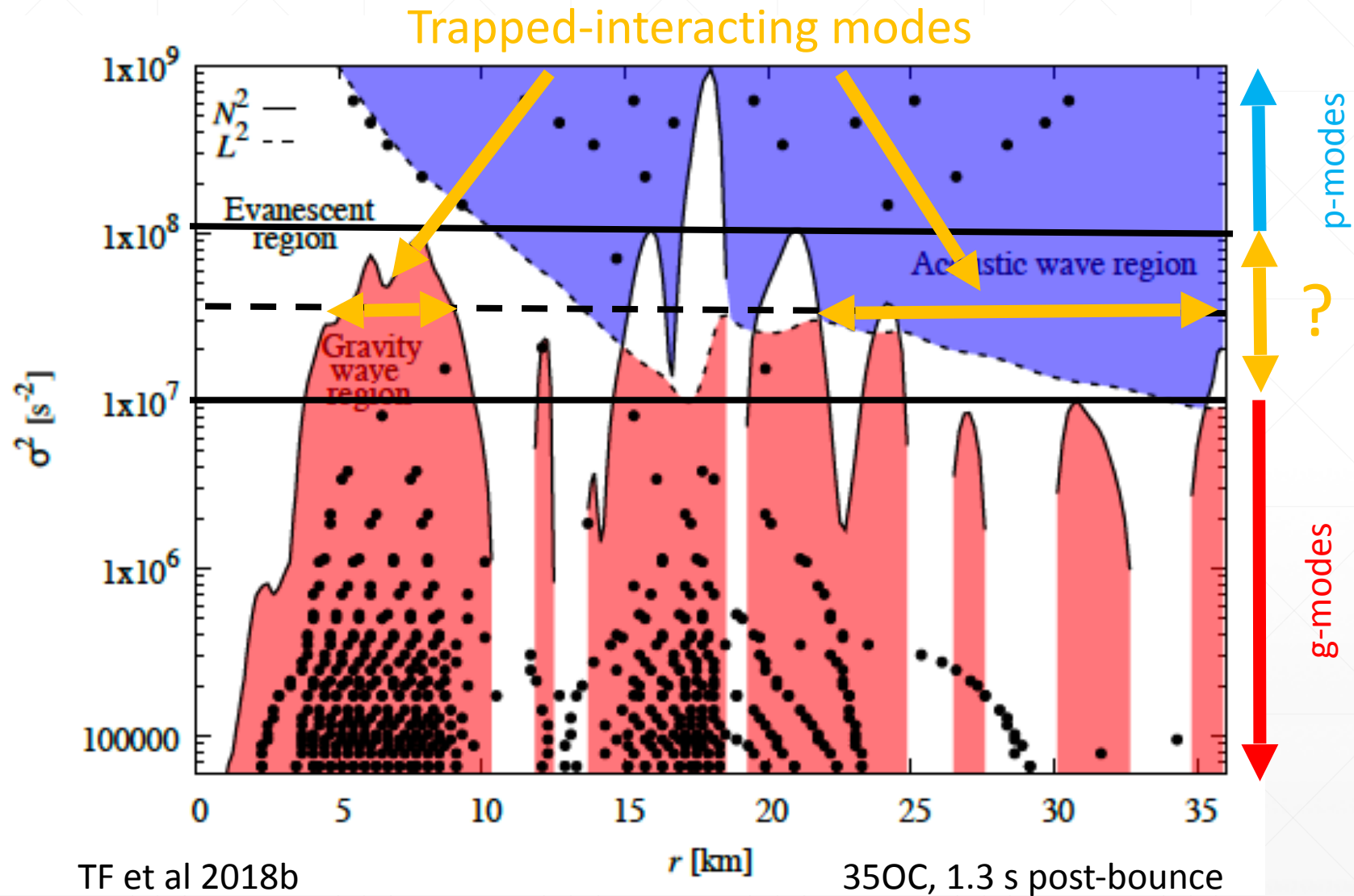


Cowling 1941 classification

p/g/f modes in real life

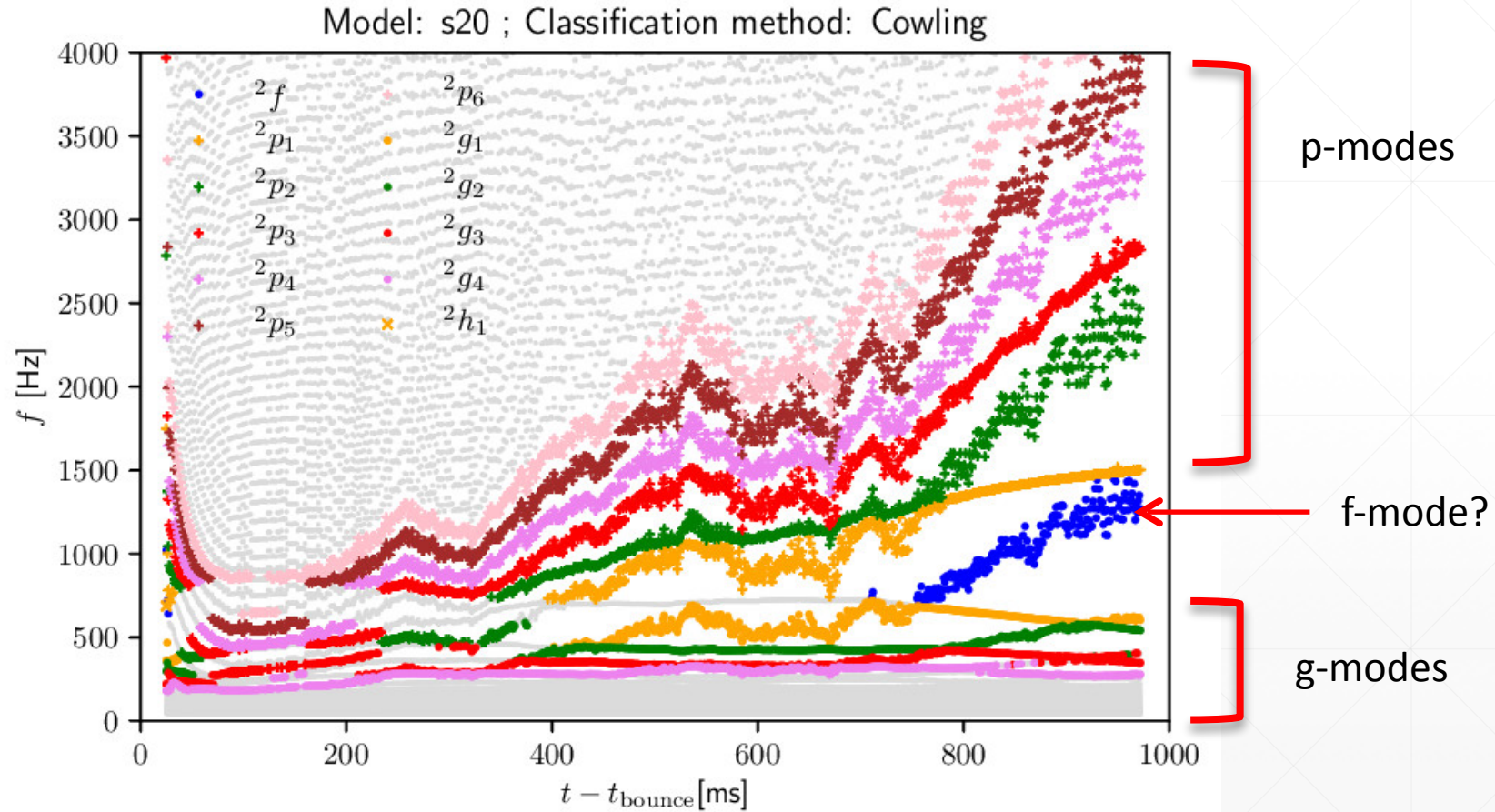


p/g/f modes in real life



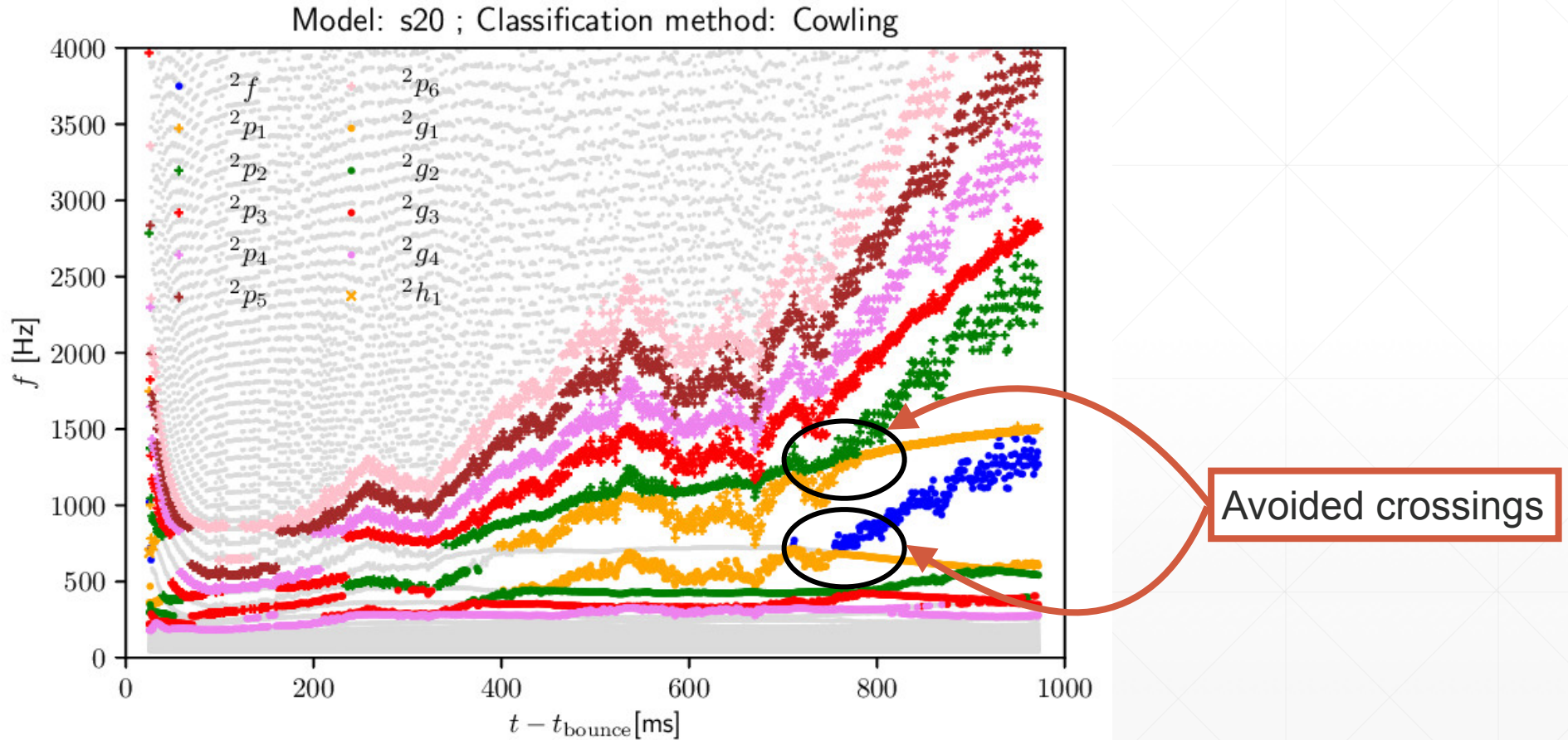
Mode classification

In TF 2018a, we perform an **automatic classification** based on the **number of nodes (n)** and on their **origin**, namely gravity modes (g-modes) and acoustic modes (p-modes).



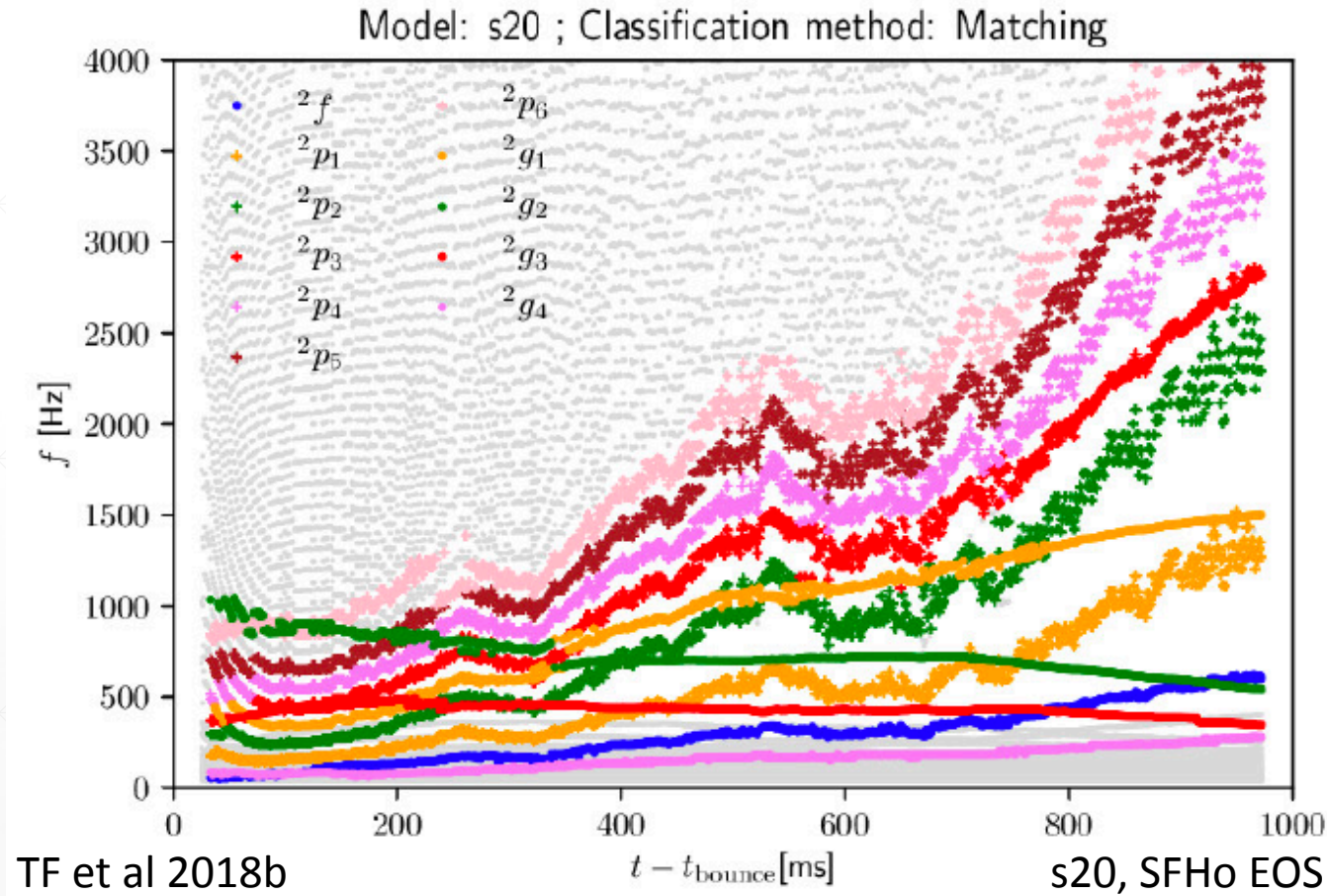
Mode classification

Avoided crossings correspond to trapped modes interacting with each other.
ESO scheme misclassifies modes across these crossings.

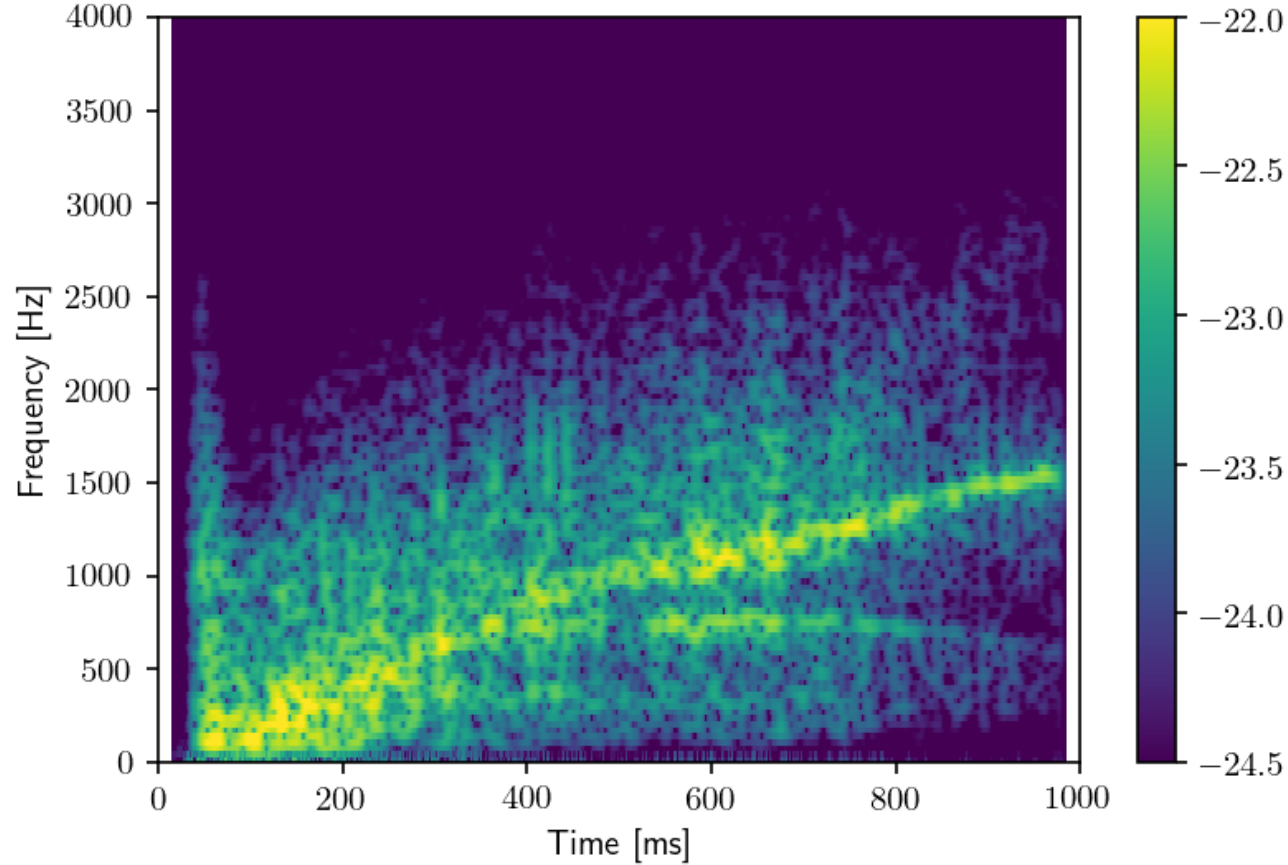


Mode classification - Matching

- Based on similarity of eigenfunctions (see Torres-Forné et al 2018b for details)
- Partially supervised (semi-automatic):



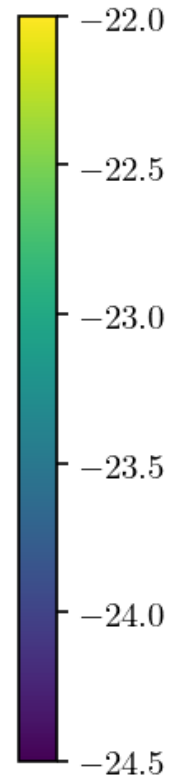
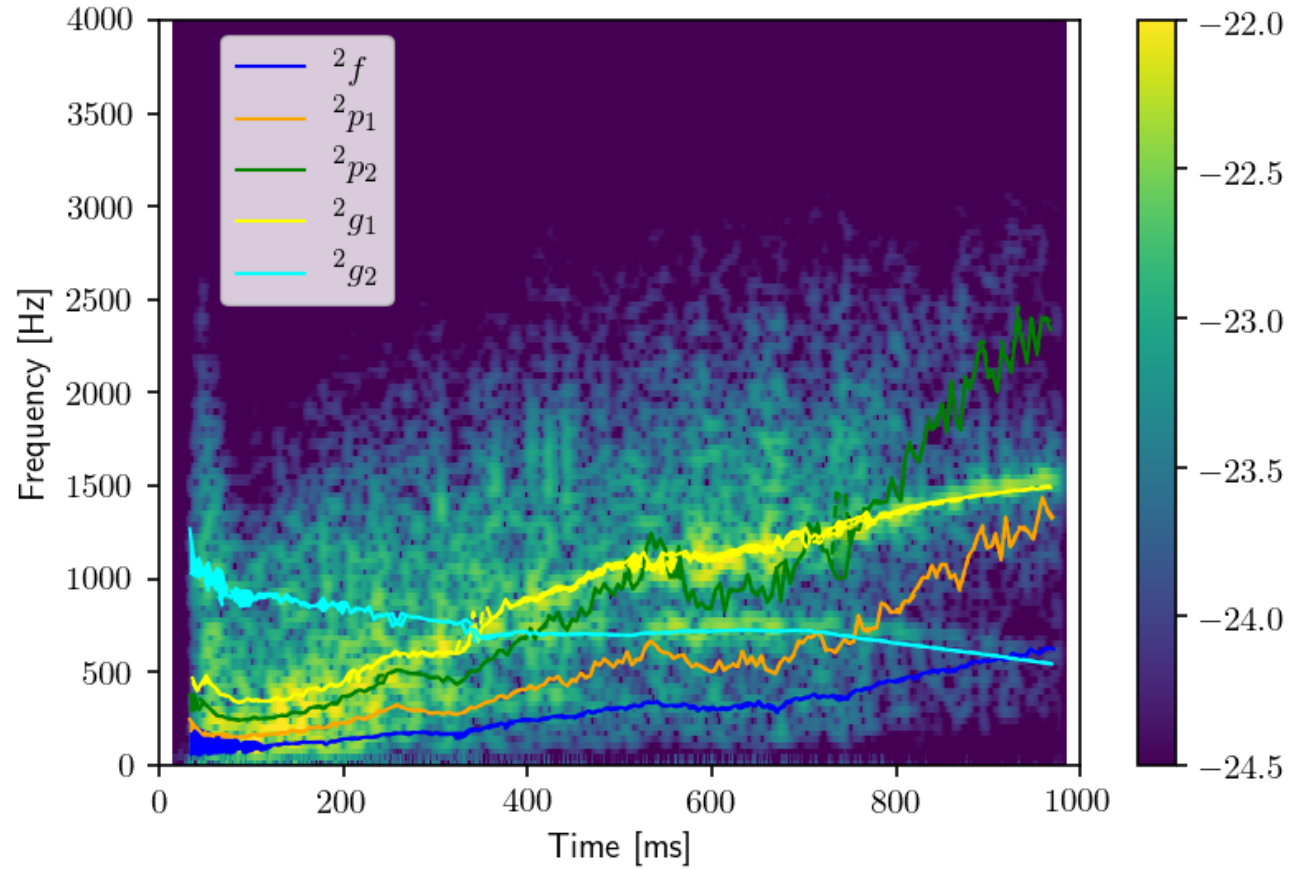
Comparison with GW emission



- Lowest-order core g-mode (2g_1) is the dominant mode
- 2g_2 also visible
- Hints of the f-mode

Lowest order modes are dominant

Comparison with GW emission



- Lowest-order core g-mode (2g_1) is the dominant mode
- 2g_2 also visible
- Hints of the f-mode

Lowest order modes are dominant

Numerical simulations

■ Derive universal relations that relate the frequencies of the most common oscillation modes observed with fundamental properties of the system.

■ We use 25 numerical simulations:

■ Two numerical codes: Aenus-Alcar (A-A) and CoCoNuT.

■ 6 Equation of State (EoS).

■ 7 different progenitors

■ Neutrino treatment:

■ A-A: algebraic Eddington factor method with an M1 closure.

■ CoCoNuT: stationary transport solution with only a one-moment closure.

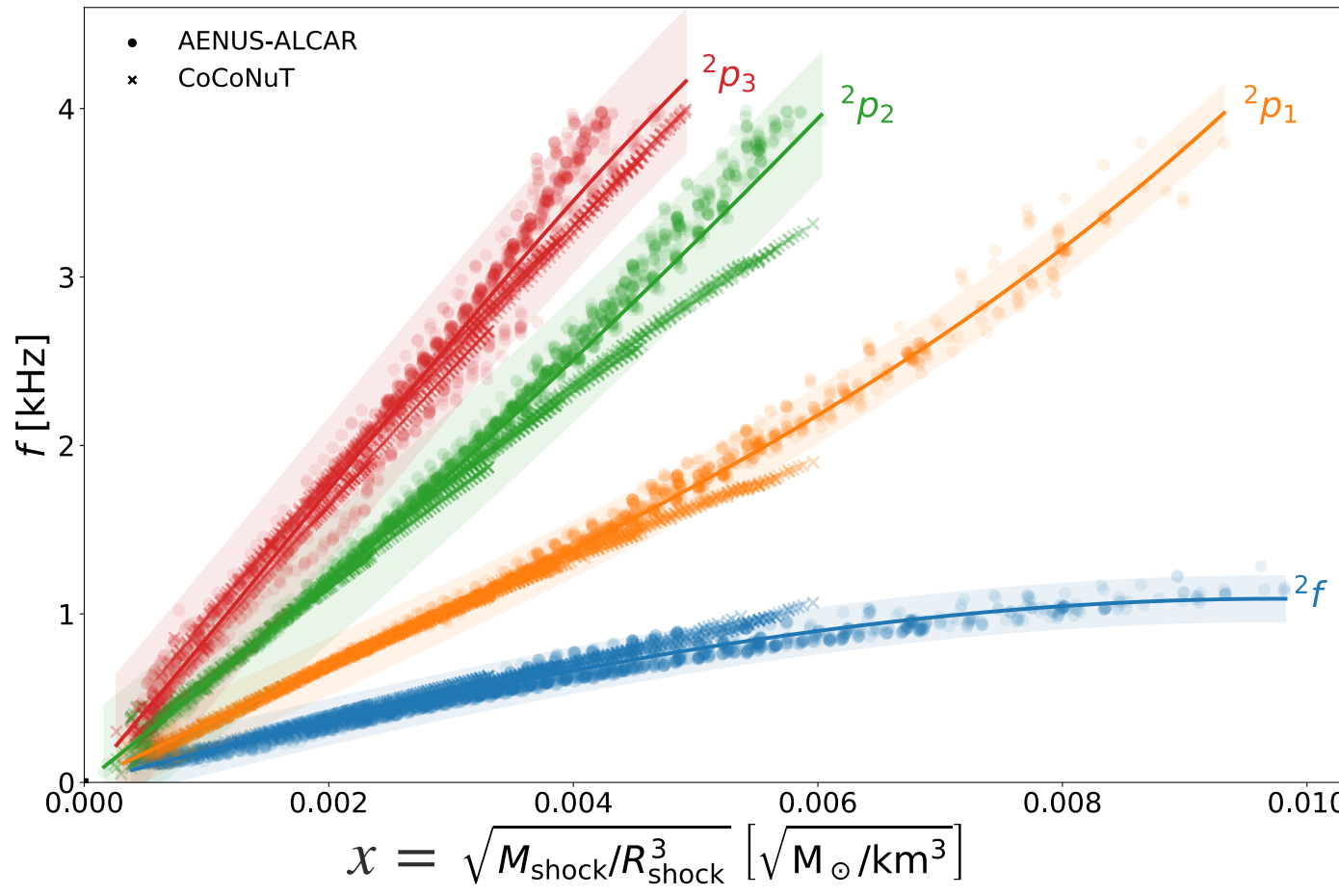
■ Gravity treatment:

■ A-A: Newtonian gravity

■ CoCoNuT: GR in the XCFC formulation

Code	Progenitor	EOS	Gravity
Aenus-ALCAR	s11.2	LS220	Newtonian
Aenus-ALCAR	s11.2	LS220	TOV-A
Aenus-ALCAR	s15	LS220	TOV-A
Aenus-ALCAR	s15	BHB-Λ	TOV-A
Aenus-ALCAR	s15	GShen-NL3	TOV-A
Aenus-ALCAR	s15	HShen	TOV-A
Aenus-ALCAR	s15	HShen-Λ	TOV-A
Aenus-ALCAR	s15	SFHo	Newtonian
Aenus-ALCAR	s20	LS220	TOV-A
Aenus-ALCAR	s20	LS220	TOV-A
Aenus-ALCAR	s25	LS220	Newtonian
Aenus-ALCAR	s25	LS220	TOV-A
Aenus-ALCAR	s25	BHB-Λ	TOV-A
Aenus-ALCAR	s30	LS220	Newtonian
Aenus-ALCAR	s30	LS220	TOV-A
Aenus-ALCAR	s40	LS220	TOV-A
Aenus-ALCAR	s75	LS220	TOV-A
Aenus-ALCAR	u20	LS220	TOV-A
CoCoNuT	s11.1	LS220	XCFC
CoCoNuT	s15	LS220	XCFC
CoCoNuT	s20	LS220	XCFC
CoCoNuT	s25	LS220	XCFC
CoCoNuT	s30	LS220	XCFC
CoCoNuT	s40	LS220	XCFC
CoCoNuT	s75	LS220	XCFC

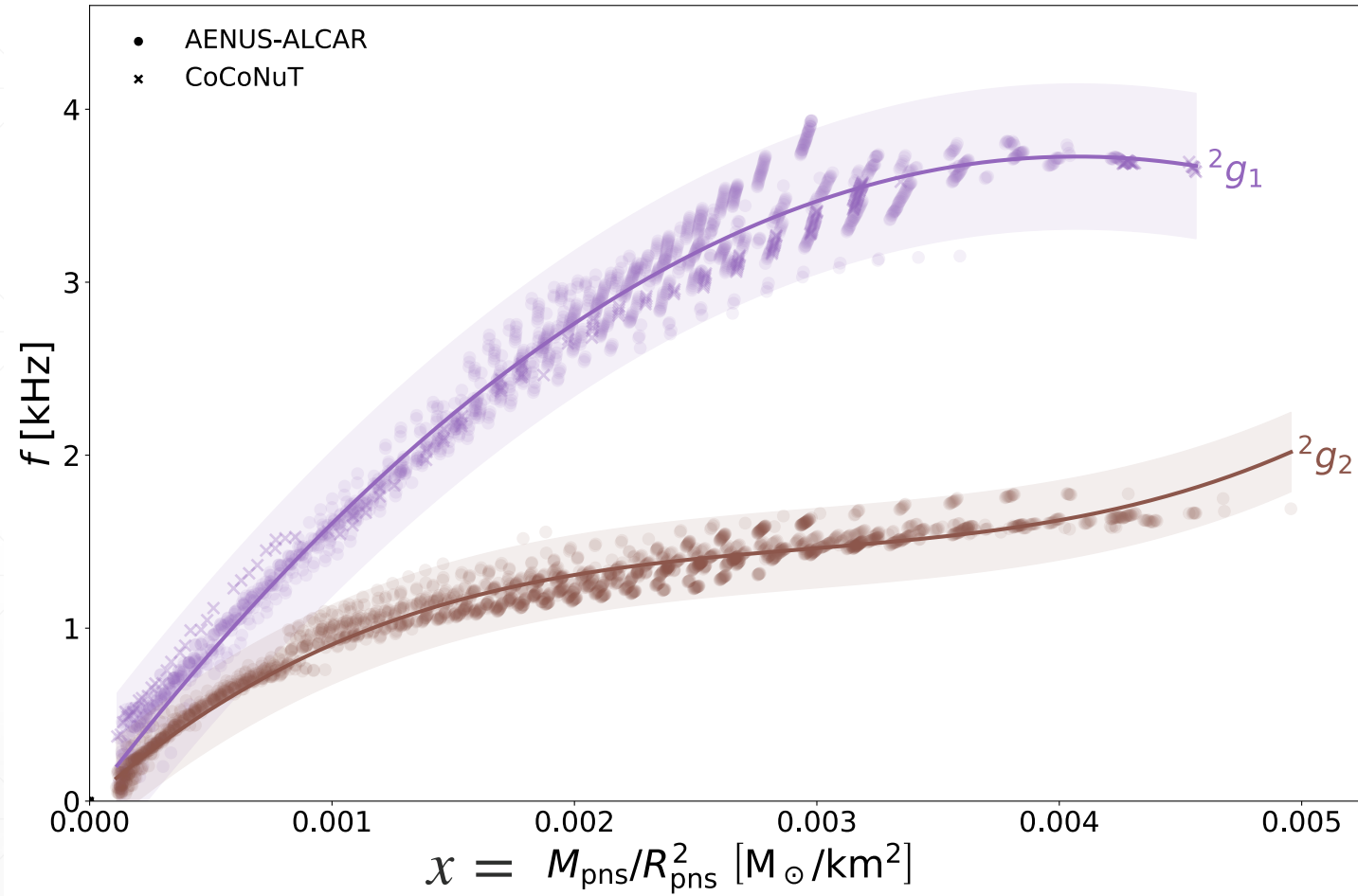
Mode fits p-modes



$$f = a + bx + cx^2 + dx^3$$

Square root of the mean density inside the shock

Mode fits g-modes



$$f = a + bx + cx^2 + dx^3$$

Surface gravity of the PNS

Mode fits - Summary

mode	x	a	$b \times 10^5$	$c \times 10^6$	$d \times 10^{10}$	R^2	σ
${}^2 f$	$\sqrt{M_{\text{shock}}/R_{\text{shock}}^3}$	-	2.00 ± 0.01	-8.5 ± 0.1	-	0.967	45
${}^2 p_1$	$\sqrt{M_{\text{shock}}/R_{\text{shock}}^3}$	-	3.12 ± 0.01	9.3 ± 0.2	-	0.991	61
${}^2 p_2$	$\sqrt{M_{\text{shock}}/R_{\text{shock}}^3}$	-	5.68 ± 0.03	14.7 ± 0.7	-	0.983	123
${}^2 p_3$	$\sqrt{M_{\text{shock}}/R_{\text{shock}}^3}$	-	8.78 ± 0.04	-4 ± 1	-	0.979	142
${}^2 g_1$	$M_{\text{pns}}/R_{\text{pns}}^2$	-	18.3 ± 0.05	-225 ± 2	-	0.982	140
${}^2 g_2$	$M_{\text{pns}}/R_{\text{pns}}^2$	-	12.4 ± 0.01	-378 ± 5	4.24 ± 0.08	0.967	76
${}^2 g_3$	$\sqrt{M_{\text{shock}}/R_{\text{shock}}^3} \ pc/\rho_C^{2.5}$	905 ± 3	-1.13 ± 0.02	2.2 ± 0.5	-	0.925	41

$$f = a + bx + cx^2 + dx^3$$

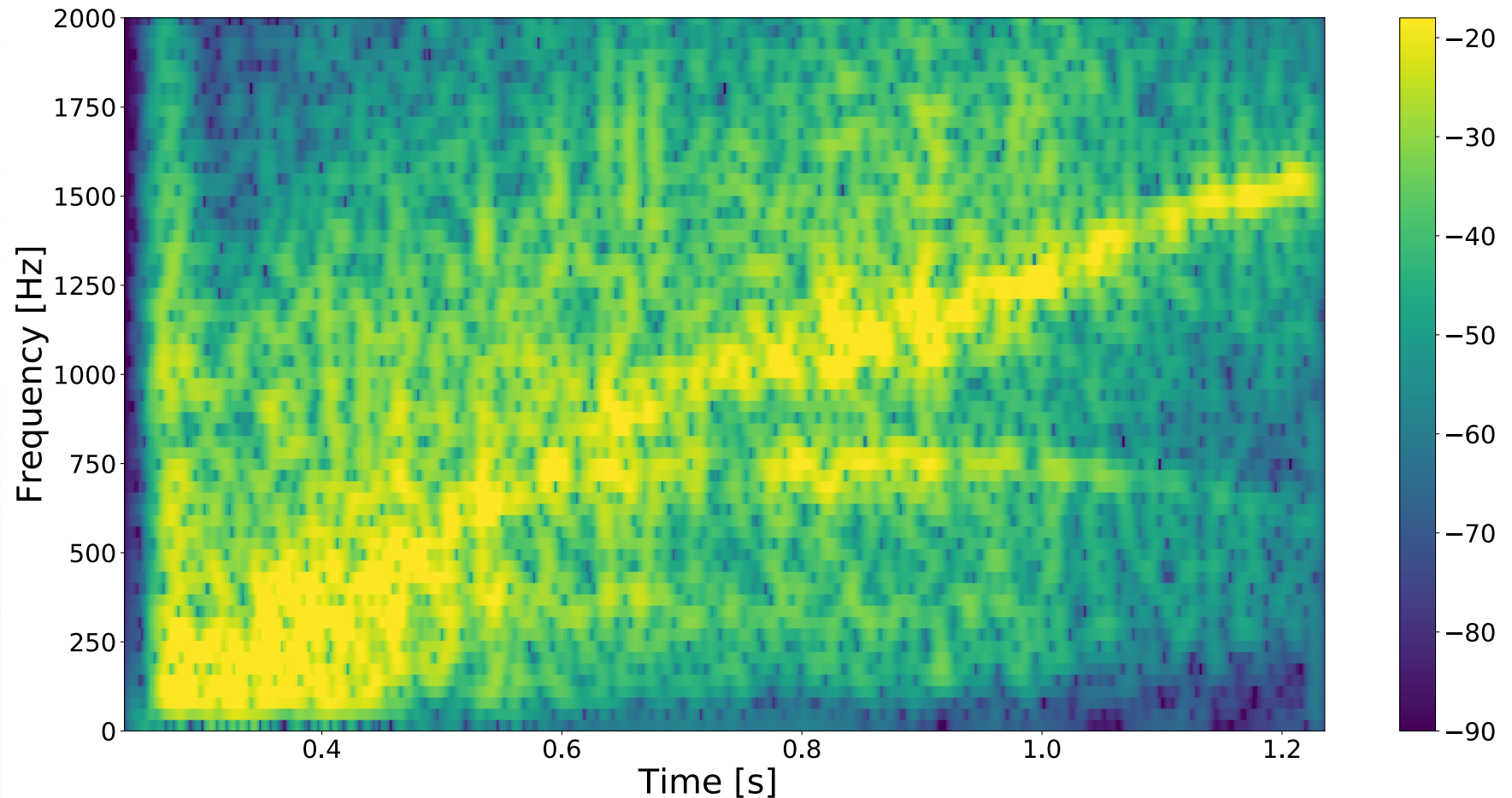
Fits compared with GW emission

Direct model: We use the fits to predict the GW emission based on a new simulation

Model s20:

- $20M_{\odot}$
- solar metallicity

2D simulation
Not used for the fits



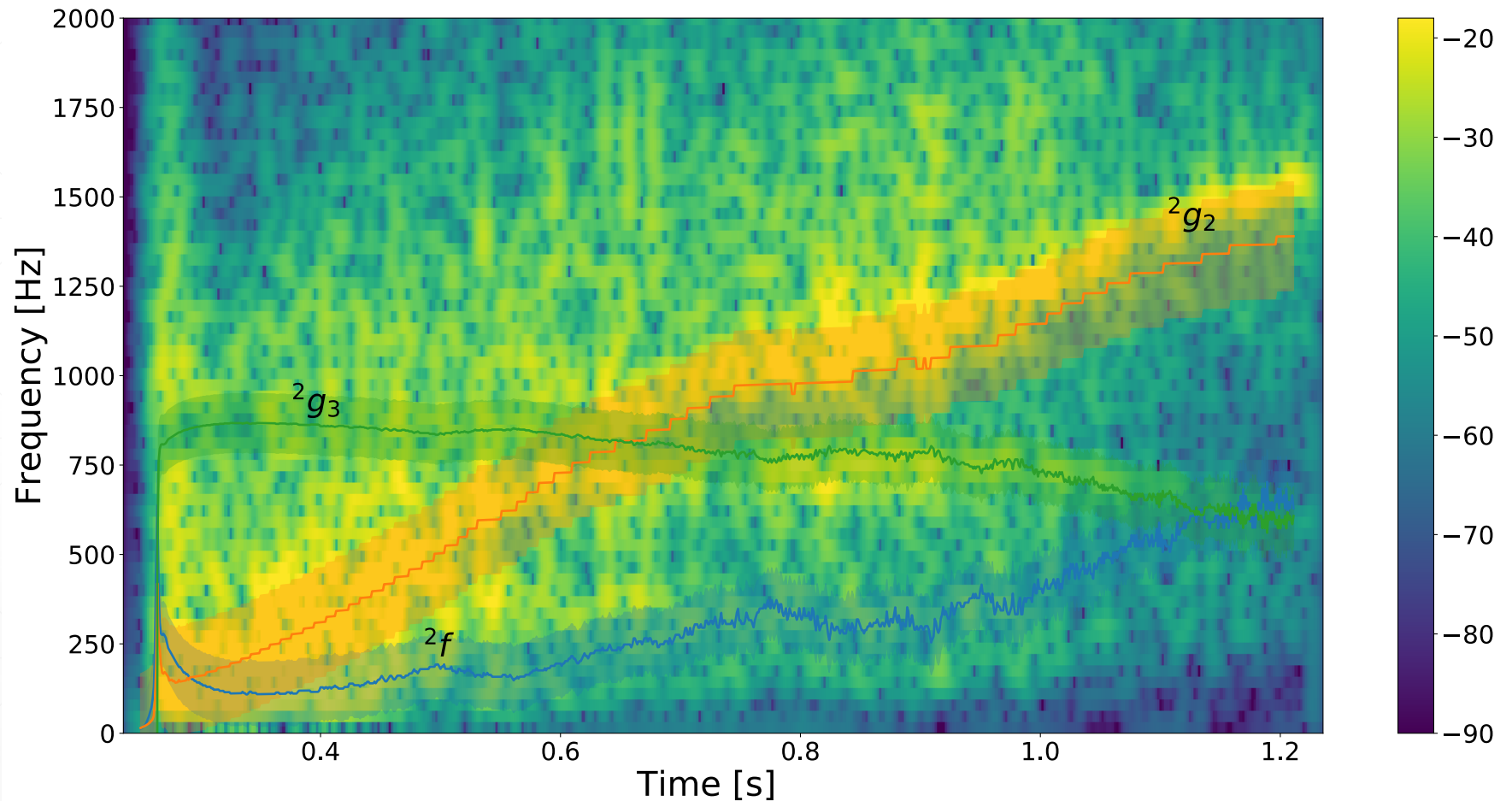
Fits compared with GW emission

Direct model: We use the fits to predict the GW emission based on a new simulation

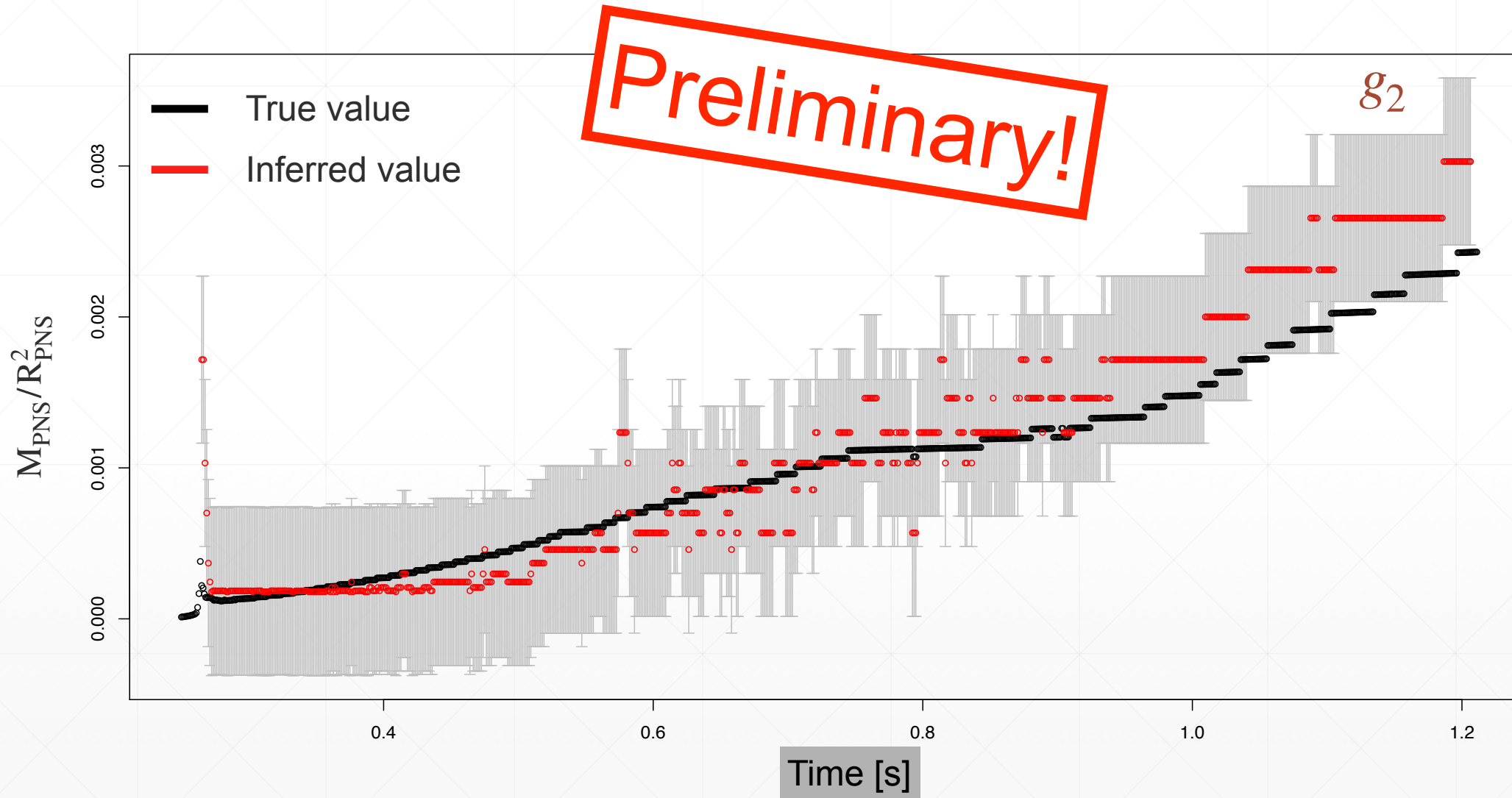
Model s20:

- $20M_{\odot}$
- solar metallicity

2D simulation
Not used for the fits



First attempt to make inference (surface gravity)



Which properties can we learn?

- Measure physical properties of a PNS during its first second of life, out of **purely GW information**.
- PNS **surface gravity** gives information about the **EoS of nuclear matter** at finite temperature. Which has not been probed yet in other astrophysical scenarios.
- Measuring **surface gravity** (g-modes) allows to constraint the **PNS radius**.
- Measuring **mean density** (f/p - modes) allows to impose constrains in the evolution of the **shock position**.

Conclusions and future work

- We have obtained a remarkably **close correspondence** with the time-frequency distribution of the gravitational-wave modes.
- GW emission in core-collapse SNe can be explained to a large degree by the excitation of PNS modes
- Mode frequencies depend on PNS properties → Universal relations
 - Independent of the EoS
 - Independent of the numerical code.
 - P-modes depend on the square root of the mean density.
 - G-modes depend on the surface gravity of the PNS
 - Rotation (small correction ~20%, even for this model)
- Future work:
 - Solve the inverse problem.
 - Improve the relations.
 - Automatic classifier.
 - Improve GREAT.

Thank you for your attention
